

Supplemental Information

Tuning Fe₂Ti distribution to enhance extrinsic magnetic properties of SmFe₁₂-based magnets

Jinbo Wei¹, Shuainan Xu¹, Chengyuan Xu¹, Xiaolian Liu¹, Yu Pan^{1*}, Wei Wang², Yue Wu², Ping
Chen², Jun Liu², Lihong Zhao¹ and Xuefeng Zhang^{1*}

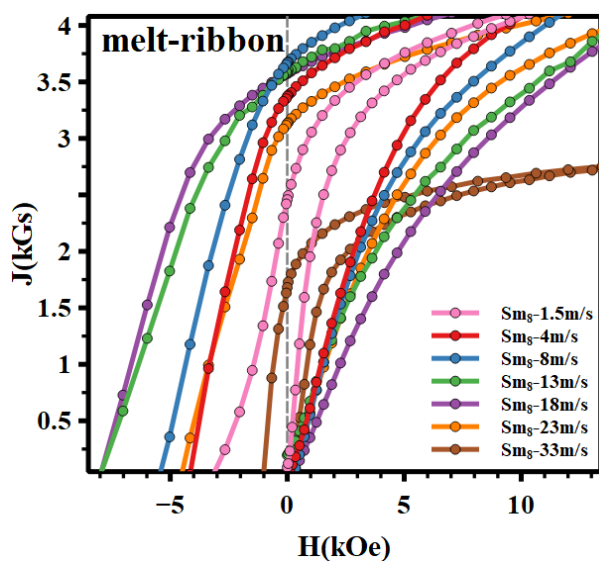


Figure S1. Demagnetization curve of the Sm₈Fe_{73.5}Ti₈V₈Al₂Ga_{0.5} alloys with different cooling rates varying from 1.5 m/s to 33 m/s.

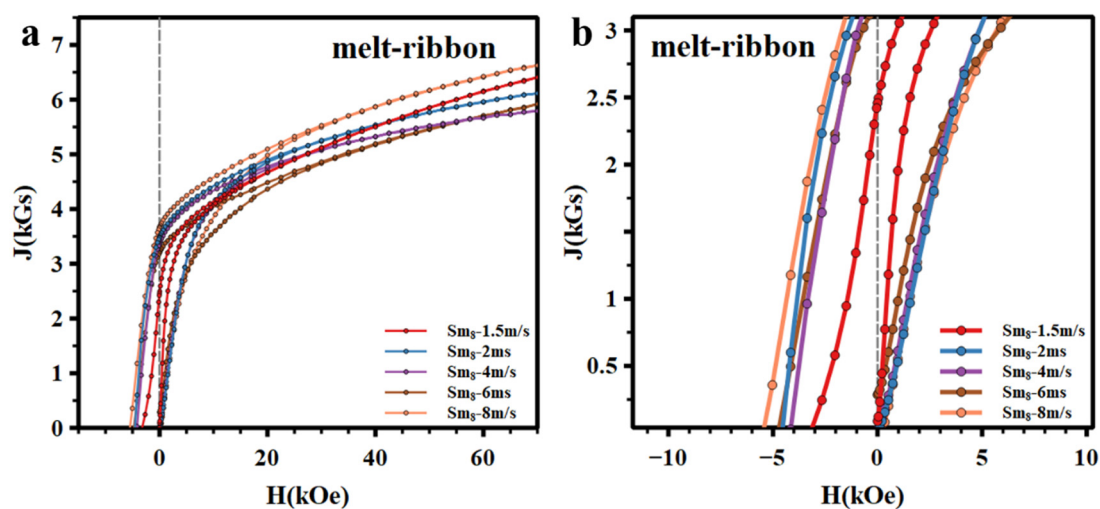


Figure S2. Demagnetization curve (a) and enlarged view of the demagnetization curves (b) of the Sm₈Fe_{73.5}Ti₈V₈Al₂Ga_{0.5} alloys with different cooling rates varying from 1.5 m/s to 8 m/s.

Table S1. Magnetic properties of the $\text{Sm}_8\text{Fe}_{73.5}\text{Ti}_8\text{V}_8\text{Al}_2\text{Ga}_{0.5}$ alloys with different cooling rates varying from 1.5 m/s to 8 m/s.

	1.5m/s	2m/s	4m/s	6m/s	8m/s
$H_c(\text{kOe})$	3.13	4.51	4.11	4.73	5.39
$M_r(\text{kGs})$	2.46	3.48	3.37	3.20	3.67

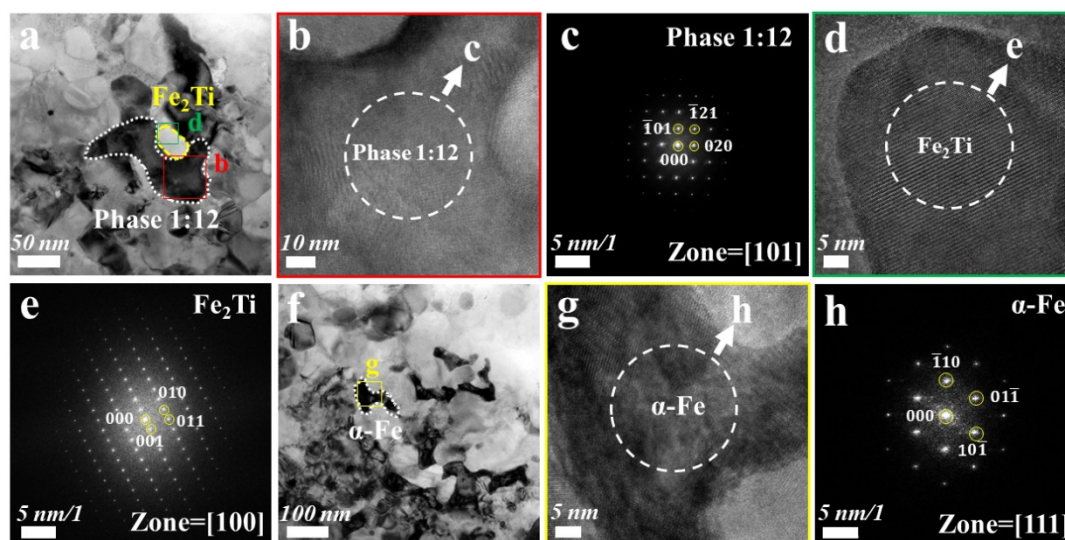


Figure S3. (a,f) TEM observation of SmFe_{12} , $\alpha\text{-Fe}$, and Fe_2Ti grains in 4m/s alloy; (b) HRTEM image for the red square region in Figure S3a; (c) SAED patterns of 1:12 phase; (d) HRTEM image for the green square region in Figure S3a; (e) SAED patterns of Fe_2Ti phase; (g) HRTEM image for the yellow square region in Figure S3f; (h) SAED patterns of $\alpha\text{-Fe}$ phase.

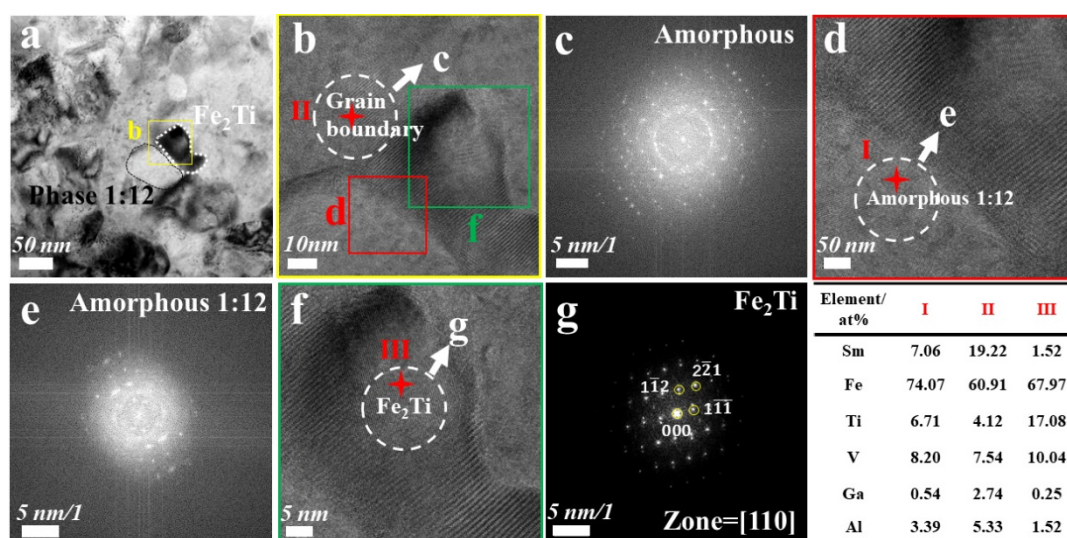


Figure S4. (a) TEM observation of SmFe_{12} and Fe_2Ti grains in 23m/s cast alloy; (b) HRTEM image for the yellow square region in Figure S4a; (c) SAED patterns of grain boundary; (d) HRTEM image for the red square region in Figure S4b; (e) SAED patterns of 1:12 phase; (f) HRTEM image for the

green square region in Figure S4b; (g) SAED patterns of Fe_2Ti phase; Point scan data at different locations.

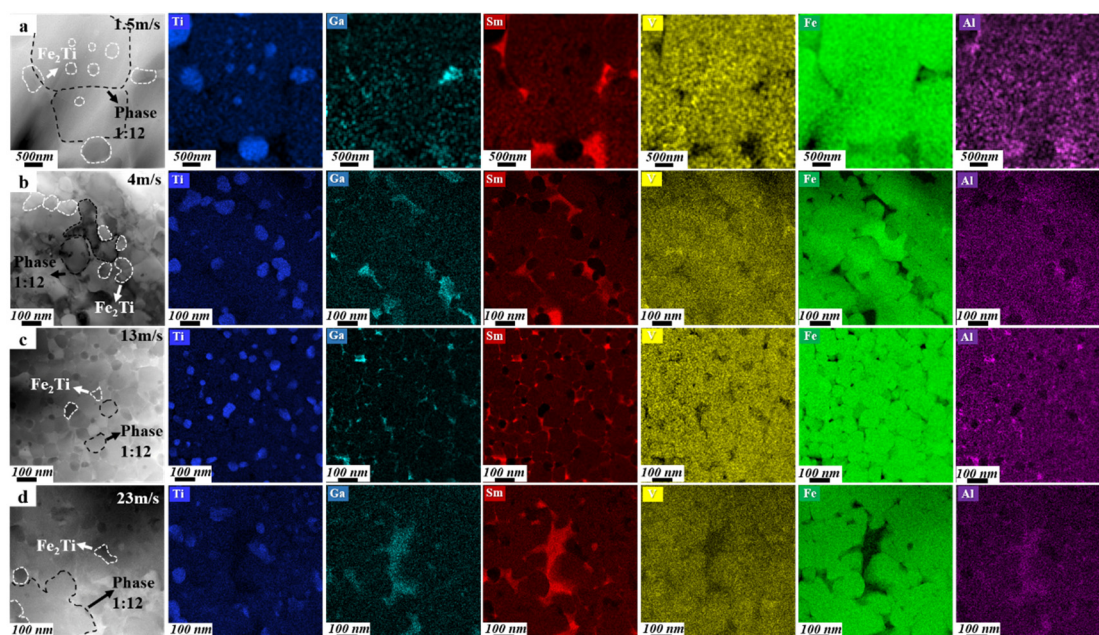


Figure S5. The HAADF image of $\text{Sm}_8\text{Fe}_{73.5}\text{Ti}_8\text{V}_8\text{Al}_2\text{Ga}_{0.5}$ alloys. (a) EDS mapping images of 1.5 m/s sample, (b) EDS mapping images of 4m/s sample, (c) EDS mapping of 13 m/s sample, and (d) EDS mapping of 23 m/s sample.

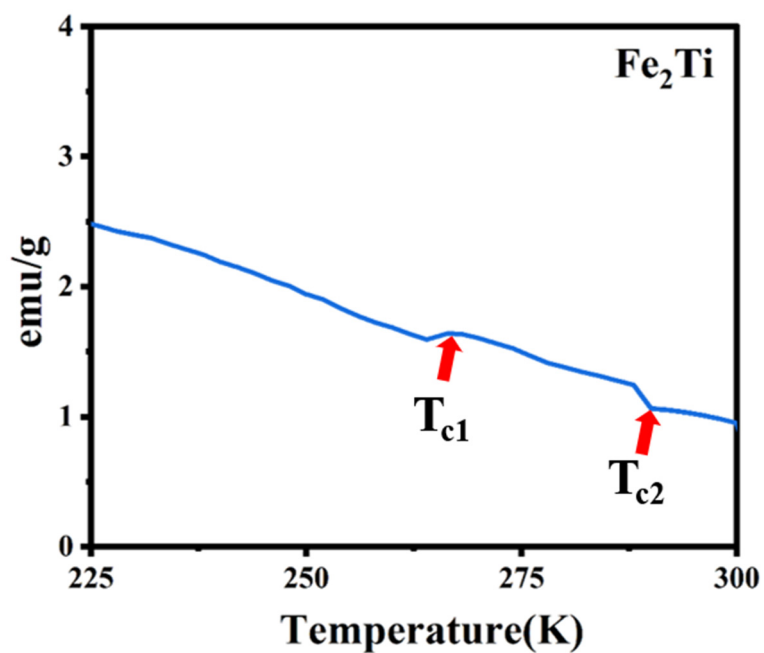


Figure S6. MT curve of Fe_2Ti .

Table S2. Anisotropy value K_u of $\text{Fe}_2(\text{Ti}_{1-x}\text{V}_x)$, $x=0\sim 1$.

	V_0	$V_{0.25}$	$V_{0.5}$	$V_{0.75}$	V_1
$K_u(\text{MJ m}^{-3})$	-0.220	-0.130	0.215	0.329	0.003
$M_{\text{cell}}(\mu_B/\text{f.u.})$	2.987	2.6685	2.371	1.972	1.463
$M_{\text{spin}}(\mu_B/\text{f.u.})$	2.874	2.542	2.198	1.802	1.329
$M_{\text{orb}}(\mu_B/\text{f.u.})$	0.113	0.143	0.173	0.170	0.134

Table S3. Comparison of coercivity data with similar work.

	<i>Highest H_c(kOe)</i>	<i>Increase in H_c(kOe)</i>
<i>Liu's work</i>	6	3
<i>Our work</i>	7.95	4.82